Quantum computing with two independent control functions: Optimal solutions to the teleportation protocol

Emanuel F. de Lima,* Marllos E. F. Fernandes, and Leonardo K. Castelano
Departamento de Física, Universidade Federal de São Carlos (UFSCar) São Carlos, São Paulo 13565-905, Brazil

(Received 27 December 2021; accepted 8 March 2022; published 30 March 2022)

A central problem in quantum computing is the finding of an unknown target state that encodes the solution of a certain computational task. To accomplish this goal, the evolution from a given initial state is performed with an associated total Hamiltonian, which is a time-dependent combination of two time-independent Hamiltonians: the problem-Hamiltonian, whose ground state is the unknown target, and a driving-Hamiltonian, whose ground state is the initial state. Here, we analyze this computational problem in the light of optimal control theory, considering each Hamiltonian modulated by an independent control function. For bounded controls, there is a minimum total evolution time beyond which the target state can be exactly prepared. We show that below this minimum time a possible optimal solution consists of both controls constantly tuned at their upper bound, provided the gradients of the associated control Hamiltonian with respect to the controls (the switching functions) are positive. We refer to this type of solution as the double-bang solution. We show that the double-bang solution is optimal for a teleportation protocol up to the minimum time. Additionally, we combine the double-bang solution and the adiabatic gate teleportation protocol to implement universal quantum computing. This approach to quantum computing is very appealing because of its simplicity and experimental feasibility. To corroborate our analytical results, we propose the use of a numerical quantum optimal control technique adapted to limit the amplitude of the controls, which converges to the double-bang solution when the final evolution time is shorter than the minimum time. We compare the fidelity of the teleported state obtained for the numerically optimized two-control functions with the usual one-control function scheme and with the quantum approximate optimization algorithm (QAOA). We find that the two-control approach has a better performance than the other approaches. Moreover, we investigate the energetic cost and the robustness against systematic errors in the teleportation protocol, considering different schemes.

DOI: 10.1103/PhysRevA.105.032454

I. INTRODUCTION

Quantum computing is currently one of the most exciting and prominent areas of physics due to its possibility of a revolutionary change in present-day technologies [1–3]. However, rather than large-scale quantum computers, we have closer at our disposal the so-called noisy intermediate-scale quantum (NISQ) devices, which can already, in principle, surpass the power of classical computers [4]. In the current NISQ era, in contrast to the standard quantum computing based on a set of logic gates, new computational paradigms have emerged based on the evolution of suitably designed Hamiltonians. For instance, variational quantum algorithms can operate in NISQ platforms to handle a variety of problems, such as ground-state chemistry, machine learning, and combinatorial optimization [5–10].

Variational quantum algorithms (VQAs) are typically based on a properly parametrized time-dependent Hamiltonian, which is applied to a register of qubits [11,12]. At the final time, the register will contain the solution for the problem. A VQA aims to solve specific problems by varying a set of parameters of the total Hamiltonian, which also parametrizes the evolution. As a special case of VQAs, quantum approximate optimization algorithms (QAOAs) have been developed for solving combinatorial optimization problems [13]. QAOA consists of applying a sequence of two unitary evolution operators originating from the so-called problem-Hamiltonian and driving-Hamiltonian in alternation, where the parameters correspond to the timings of these unitary operators.

Adiabatic quantum algorithms (AQAs) are also in the class of quantum computing approaches that are based on a time-dependent combination of time-independent Hamiltonians [14,15]. AQAs exploit the fact that a quantum system remains in its ground state if the evolution is made sufficiently slow. In this approach, the total Hamiltonian changes adiabatically from the driving-Hamiltonian to the problem-Hamiltonian, whose ground state encodes the solution of the computational problem. However, the time required to keep the adiabatic condition valid can be too long to be useful in practical situations. Several alternatives have been proposed to circumvent this problem, such as the local adiabatic evolution or the use of counterdiabatic drivings [16,17]. Related to AQA, the method of quantum annealing (QA) emerged as a quantum version of the classical optimization technique of simulated annealing [18–21]. As in AQA, the connection of the driving Hamiltonian to the problem Hamiltonian in QA is

*emanuel@df.ufscar.br

carried out through a smooth continuous function of time, but allowing for faster, nonadiabatic dynamics.

Recently, several works explored connections of optimal control theory with VQA and also with QA [22–25]. In Ref. [26], it was argued that for a fixed time, square pulse controls (bang-bang type) are optimal, giving support to the QAOA methodology. However, from the standard form of QA involving a single control function, the authors of Ref. [27] showed that a more general form of the optimal solution is of "bang-annealing-bang" type, meaning that a hybrid time-dependent control starting at the minimum allowed value and ending at the maximum possible value, with a smooth annealing segment in between is usually optimal. In Ref. [28], a comprehensive perspective of the possible connections between VQA with quantum control was presented. Specifically, the authors indicated that the quantum optimal theory background can extract a rich variational structure of VQA and provide a better understanding of variational experiments.

In this paper, we analyze the problem of finding an unknown target state that encodes the solution of a certain computational task in the framework of optimal control theory. The evolution of the system is governed by a combination of a driving and a problem Hamiltonians, each one modulated by an independent control function. For bounded controls, we find two regimes depending on the total evolution time: (i) for sufficiently long times, optimal solutions exist such that the target ground state can be exactly obtained; (ii) for short times, optimal solutions cannot fully prepare the target state. The minimum time is the least total evolution time for which the target state can be exactly prepared. If the gradients of the associated control Hamiltonian with respect to the controls (switching functions) are positive and the final evolution time is shorter than the minimum time, we demonstrate that the optimal solution is obtained by simply setting both control functions at their maximum values during the entire evolution. We call this kind of solution the double-bang solution. The main difference of our findings when compared to those obtained in Refs. [26,27] is that we explicitly formulate the control problem considering two independent control functions, which leads to the double-bang solution.

Universal quantum computer can be achieved through the adiabatic gate teleportation (AGT) protocol [29], although the adiabatic evolution is slow and requests a route to speed up the time evolution [30]. By using the double-bang solution, we show how to implement universal quantum computing by means of AGT in the fastest way. In other words, universal quantum computing can be performed by switching on the driving and the problem Hamiltonians of the AGT scheme. Particularly, the minimum time for the AGT is the time where the mean value of the problem Hamiltonian reaches its ground state with the double-bang solution; thereby, accomplishing the computational task with practically full accuracy.

II. CONTROL PROBLEM

Consider that we are given two time-independent Hamiltonians: H_0 (driving) and H_1 (problem), with $|\phi_0\rangle$ being the ground state of H_0 with eigenvalue E_0^0, and $|\chi_0\rangle$ the ground state of H_1 with eigenvalue E_0^1. Suppose that the system is initially prepared in the ground state of H_0, $|\psi(t=0)\rangle = |\phi_0\rangle$, and evolves according to the total time-dependent Hamiltonian

$$H(t) = \varepsilon_0(t)H_0 + \varepsilon_1(t)H_1, \tag{1}$$

where $\varepsilon_0(t)$ and $\varepsilon_1(t)$ are two independent control functions.

We seek to find the controls $\varepsilon_0^*(t)$ and $\varepsilon_1^*(t)$ that maximize the expectation value of a given observable O at the final time $t = T$, expressed as a functional of the controls

$$J[\varepsilon_0, \varepsilon_1] = \langle O(T)\rangle \equiv \langle\psi(T)|O|\psi(T)\rangle, \tag{2}$$

while limiting the amplitudes of the controls such that $0 \leqslant \varepsilon_k \leqslant 1$, $k = 0, 1$. The maximum possible value of J is given by the largest eigenvalue of O, which we simply designate by $J_{\max}$.

We point out that in the standard versions of adiabatic or annealing quantum computing, the controls ε_k are not independent, being related by $\varepsilon_1(t) = 1 - \varepsilon_0(t)$, while the observable is usually the negative of the problem Hamiltonian $O = -H_1$ (equivalently, the problem can be recast as the minimization of H_1). Moreover, by the adiabatic theorem, it is known that an optimal solution to the control problem exists for sufficiently long final times T, in which case $J_{\max}$ can be obtained.

Necessary conditions for optimal solutions to the present control problem can be obtained by means of the calculus of variations [31]. In this approach, an augmented functional J_a is formed from Eq. (2), incorporating the Schrödinger equation with the help of a Lagrange multiplier. The vanishing of the variation of the augmented functional $\delta J_a = 0$ leads to necessary conditions for optimality. Alternatively, in the spirit of Pontryagin's formulation, it is also possible to obtain these necessary conditions using the so-called control Hamiltonian function, which can be obtained by a Legendre transformation from the variational formalism (see Refs. [27,32] for further details). Thus, for convenience, we consider the problem in terms of the control Hamiltonian $\mathcal{H}$ [not to be confused with the system Hamiltonian $H(t)$] given by [33,34],

$$\mathcal{H}(\psi, \lambda, \varepsilon_0, \varepsilon_1, t) = -\mathrm{i}\langle\lambda(t)|H(t)|\psi(t)\rangle + \mathrm{c.c.}, \tag{3}$$

where $|\lambda(t)\rangle$ is an auxiliary adjoint vector state. Hereafter, we adopt $\hbar = 1$.

Substituting Eq. (1) into Eq. (3), we obtain

$$\mathcal{H}(\psi, \lambda, \varepsilon_0, \varepsilon_1, t) = \varepsilon_0(t)\Phi_0(t) + \varepsilon_1(t)\Phi_1(t), \tag{4}$$

where the gradients with respect to the controls (also called switching functions) are

$$\Phi_k(t) \equiv 2\,\mathrm{Im}\,\{\langle\lambda(t)|H_k|\psi(t)\rangle\}, \quad k = 0, 1. \tag{5}$$

According to the Pontryagin's maximum principle, necessary conditions for an optimal solution are given by the evolution of the state and the adjoint vectors

$$|\dot{\psi}(t)\rangle = -iH(t)|\psi(t)\rangle, \ |\psi(0)\rangle = |\phi_0\rangle, \tag{6a}$$

$$|\dot{\lambda}(t)\rangle = -iH(t)|\lambda(t)\rangle, \ |\lambda(T)\rangle = O|\psi(T)\rangle, \tag{6b}$$

along with the maximum condition of the control Hamiltonian

$$\mathcal{H}(\psi^*, \lambda^*, \varepsilon_0^*, \varepsilon_1^*, t) \geqslant \mathcal{H}(\psi^*, \lambda^*, \varepsilon_0, \varepsilon_1, t), \quad \forall \text{ admissible } \varepsilon_0,\ \varepsilon_1, \tag{7}$$

where the symbol $*$ refers to the dynamical quantities calculated at an optimal solution.

Considering admissible variations $\delta\varepsilon_k$ around the optimal solution $\varepsilon_k(t) = \varepsilon_k^*(t) + \delta\varepsilon_k(t)$, Eq. (7) yields

$$\frac{\partial\mathcal{H}(\varepsilon_k^*)}{\partial\varepsilon_k}\delta\varepsilon_k(t) = \Phi_k^*(t)\delta\varepsilon_k(t) \leqslant 0, \quad k = 0, 1. \tag{8}$$

Although Eq. (8) can be viewed as a weaker form of the Pontryagin's principle than Eq. (7), it also furnishes the necessary conditions for optimality. Thus, for each value of k and for a given t, three situations can occur: (i) $\Phi_k^*(t) = 0$, (ii) $\Phi_k^*(t) > 0$ and $\delta\varepsilon_k(t) < 0$, or (iii) $\Phi_k^*(t) < 0$ and $\delta\varepsilon_k(t) > 0$. Note that $\delta\varepsilon_k(t) < 0$ for all admissible variations implies $\varepsilon_k^*(t) = 1$ because the variations about the maximum value must be negative, while $\delta\varepsilon_k(t) > 0$ implies $\varepsilon_k^*(t) = 0$ because the variations about the minimum must be positive. As is usually termed in optimal control theory [31], a singular interval occurs when the gradients vanish simultaneously in a finite interval of time, $\Phi_0^*(t) = \Phi_1^*(t) = 0$. As explained below, we will tacitly assume in the following that singular intervals do not occur by considering sufficiently short final times.

It is straightforward to verify that $\varepsilon_0(t)\dot{\Phi}_0 = -\varepsilon_1(t)\dot{\Phi}_1$ and, as a consequence, the time derivative of the control Hamiltonian is given by

$$\frac{d\mathcal{H}(t)}{dt} = \dot{\varepsilon}_0(t)\Phi_0 + \dot{\varepsilon}_1(t)\Phi_1. \tag{9}$$

For optimal solutions, either the control is constant, $\dot{\varepsilon}_k^*(t) = 0$, or the gradient vanishes, $\Phi_k^*(t) = 0$, which implies that the control Hamiltonian calculated at an optimum trajectory $\mathcal{H}^*$ is a constant of motion. Moreover, when the amplitudes of optimal controls are within the boundaries $0 < \varepsilon_k^*(t) < 1$, for all $t \in [0, T]$, the situation is similar to the unbound control problem: necessarily the gradients are null and the control Hamiltonian vanishes identically $\mathcal{H}^* = 0$.

The necessary conditions for an optimal solution evidence that, when the final time T is long enough, there are optimal solutions such that the control Hamiltonian $\mathcal{H}^*$ is null and the maximum possible value of the functional Eq. (2), $J_{\max}$, can be reached. On the other hand, below a certain minimum value $T_{\min}$ of the evolution time $J_{\max}$ cannot be reached. In this case, $T < T_{\min}$, the control Hamiltonian at the optimal solution, is a positive constant.

To show this, following the reasoning of the authors of Ref. [27], consider that the final time T of the control problem is free and set a new cost functional J' given by

$$J'[\varepsilon_0, \varepsilon_1, T] = J[\varepsilon_0, \varepsilon_1] - \alpha T, \tag{10}$$

where $\alpha \geqslant 0$ is a given positive constant. The functional to be maximized, J', has a penalty term to account for increasing the final time. We can associate the same control Hamiltonian in Eq. (4) to this free final-time cost functional, along with Eqs. (6) and (7), and the additional necessary condition

$$\mathcal{H}^*(T) = \alpha. \tag{11}$$

For $\alpha = 0$, corresponding to a free final time with no penalty term, the control Hamiltonian calculated at an optimal solution vanishes for all times and J'^* assumes its maximum possible value $J'^* = J_{\max}$. In this case, there will be a sufficiently long final time such that we can find optimal solutions such that the controls are within the boundaries. However, for $\alpha \neq 0$, the control Hamiltonian at an optimal solution is a positive constant α and $J_{\max}$ is not obtained. A thorough analysis of these results was recently presented in Ref. [34].

Returning to the problem with a fixed final time, consider the case where $T < T_{\min}$, meaning that the gradients $\Phi_k(t)$ do not vanish simultaneously and $\mathcal{H}^*(T) = \text{constant} > 0$. Note that the value of the control Hamiltonian at an optimal solution depends exclusively on the final time T. Now set $O = -H_1$, which leads to $J^*(T) < -E_0^1 = J_{\max}$. Additionally, from Eqs. (6a), (6b), and (5), we obtain

$$\begin{aligned}\Phi_1^*(T) &= 2\,\mathrm{Im}\,\{\langle\lambda^*(T)|H_1|\psi^*(T)\rangle\} \\ &= -2\,\mathrm{Im}\left\{\langle\psi^*(T)|H_1^2|\psi^*(T)\rangle\right\} = 0,\end{aligned} \tag{12}$$

and

$$\begin{aligned}\Phi_0^*(0) &= 2\,\mathrm{Im}\,\{\langle\lambda^*(0)|H_0|\psi^*(0)\rangle\} \\ &= 2E_0^0\,\mathrm{Im}\,\{\langle\lambda^*(0)|\psi^*(0)\rangle\} \\ &= -2E_0^0\,\mathrm{Im}\,\{\langle\psi^*(T)|H_1|\psi^*(T)\rangle\} = 0,\end{aligned} \tag{13}$$

where we used the fact that $\frac{d}{dt}\langle\lambda^*(t)|\psi^*(t)\rangle = 0$.

Thus, we conclude that

$$\mathcal{H}^*(T) = \varepsilon_0^*(T)\Phi_0^*(T) = \varepsilon_1^*(0)\Phi_1^*(0). \tag{14}$$

Further, since $\mathcal{H}^*(T)$ is positive, $\Phi_0^*(T) > 0$ and $\Phi_1^*(0) > 0$. Consequently, from Eq. (8), we must have $\varepsilon_0^*(T) = \varepsilon_1^*(0) = 1$ and $\mathcal{H}^*(T) = \Phi_0^*(T) = \Phi_1^*(0)$. We note that, differently from the case of single control [27], the fact that $\varepsilon_0^*(T) = 1$ and $\varepsilon_1^*(0) = 1$ does not impose any condition on $\varepsilon_0^*(0)$ and $\varepsilon_1^*(T)$.

The set of necessary conditions deduced so far helps to single out candidates for optimal solutions. Here we select such a candidate that we name the double-bang solution, consisting of both controls set to their (equal) maximum values $\varepsilon_0(t) = \varepsilon_1(t) = 1\ \forall t \in [0, T]$. Clearly, such a solution satisfies the boundary condition just derived $\varepsilon_0(T) = 1$ and $\varepsilon_1(0) = 1$. Moreover, assuming that both gradients are positive for $\varepsilon_0(t) = \varepsilon_1(t) = 1$, then the double-bang solution also meets Eq. (8). Additionally, the control Hamiltonian is given by $\mathcal{H}(T) = \Phi_0(t) + \Phi_1(t)$. Noting that the time derivative of the sum of the gradients can be written as $\frac{d}{dt}[\Phi_0(t) + \Phi_1(t)] = [\varepsilon_0(t) - \varepsilon_1(t)]\xi(t)$, where $\xi(t) = 2\,\mathrm{Re}\{\langle\dot{\lambda}(t)|[H_1, H_0]|\psi(t)\rangle\}$, we perceive that the control Hamiltonian is constant for the double-bang solution. The conditions for the gradients being nonnegative are problem-specific since they depend essentially on the Hamiltonians H_0 and H_1. However, we will show in the following that the gradients are nonnegative for a teleportation protocol, and consequently the double-bang solution is optimal up to the minimum time, which allows for universal quantum computing.

It is worth comparing the yield for the same final time T obtained with two-control functions with that of the standard QA scheme, which employs a single control function such that $\varepsilon_1(t) = 1 - \varepsilon_0(t)$. In particular, if an optimal solution for the two-control case is given by the double-bang solution, then, from Eq. (7), an optimal solution for the one-control case is, in general, a suboptimal solution for the two-control case.

III. TBQCP OPTIMIZATION METHOD

Numerically, the optimal controls are sought by the two-point boundary-value quantum control paradigma (TBQCP) [35], which we adapted to limit the amplitudes of the control functions. The TBQCP technique was employed to study the protocols related to standard-gate quantum computing with great efficiency, e.g., to compute optimal controls capable of implementing the universal set of quantum gates in double quantum dots [36] or the permutation algorithm in hybrid qubits [37].

The TBQCP is an iterative monotonic method able to find optimal controls that, given an initial state $|\psi(t=0)\rangle \equiv |\psi_0\rangle$, maximize the expectation value of a physical observable O at the final time T. Starting with some trial controls, the physical observable is evolved backwards (from the final time $t=T$ to the initial time $t=0$) through the following equation:

$$i\frac{\partial O^{(n)}(t)}{\partial t} = \left[O^{(n)}(t),\, H^{(n)}(t)\right],\; O(T) \to O(0), \tag{15}$$

where $H^{(n)}(t) = \sum_{k=0}^{1} \varepsilon_k^{(n)}(t) H_k$ and $\varepsilon_k^{(n)}(t)$ are the controls in the nth iteration. The initial state $|\psi_0\rangle$ is evolved forward with the Schrödinger equation

$$i\frac{\partial |\psi^{(n+1)}(t)\rangle}{\partial t} = H^{(n+1)}(t)|\psi^{(n+1)}(t)\rangle, \tag{16}$$

where $H^{(n+1)}(t) = \sum_{k=0}^{1} \varepsilon_k^{(n+1)}(t) H_k$ and $\varepsilon_k^{(n+1)}(t)$ is the $(n+1)$st iteration control for $k=0,1$, which is calculated through the following expression:

$$\varepsilon_k^{(n+1)}(t) = \varepsilon_k^{(n)}(t) + \eta f_k^{(n+1)}(t),\; k=0,1, \tag{17}$$

where η is a positive constant and the control correction is given by

$$f_k^{(n+1)}(t) = 2\mathrm{Im}\{\langle\psi^{(n+1)}(t)|O^{(n)}(t)H_k|\psi^{(n+1)}(t)\rangle\}, \tag{18}$$

where $k=0,1$. It was shown that, as an optimal solution is approaching, the control correction $f_k^{(n+1)}(t)$ is equivalent to the gradient $\Phi_k(t)$ (Eq. (5) [35]), which establishes a close connection between the TBQCP and the variational version of the optimal control theory. Equations (15) to (17) are solved in a self-consistent way, starting with trial controls $\varepsilon_k^{(0)}(t)$ $(k=0,1)$ and monotonically increasing the value of the desired physical observable $\langle O(T)\rangle = \langle\psi(T)|O(T)|\psi(T)\rangle$, see more details in Ref. [35]. In addition, at each iteration step, the amplitudes of the controls are bounded to the interval [0,1] by enforcing the value of the corresponding limit whenever the control transcends the bounds of the interval [0,1] in Eq. (17). In this case, if the control function $\varepsilon_k^{(0)}(t)$ $(k=0,1)$ exceeds one of the bounds 0 or 1 in a certain time interval, its value is set equal to the crossed bound in this same time interval during the entire self-consistent calculation.

IV. QUANTUM APPROXIMATE OPTIMIZATION ALGORITHM

To compare with the optimized solutions of the control problem, we also consider the QAOA approach. In the spirit of VQAs, the QAOA ansatz consists of alternately switching on each Hamiltonian H_k $(k=0,1)$ in a certain time interval, while the other one is switched off. Thus, the time evolution becomes

$$|\psi(t)\rangle = U(H_0,\beta_p)U(H_1,\gamma_p)\ldots U(H_0,\beta_1)U(H_1,\gamma_1)|\psi(0)\rangle, \tag{19}$$

where $U(H_0,\beta_j) = \exp(-\mathrm{i}H_0\beta_j)$ and $U(H_1,\gamma_j) = \exp(-\mathrm{i}H_1\gamma_j)$ are evolution operators. β_j and γ_j are real positive variational parameters that should be adjusted to maximize the expectation value of an observable O at the final time $t=T$, $\langle O(T)\rangle$. The variational parameters are constrained such that $T = \sum_{j=1}^{p}(\gamma_j+\beta_j)$, where p specifies the quantity of shifts from one Hamiltonian to the other. By construction, QAOA provides a solution to the control problem such that the controls satisfy $\varepsilon_1(t) = 1-\varepsilon_0(t)$ and $\varepsilon_0(t)$ is of bang-bang type, meaning that the control is turned on and off (possibly many times) during the evolution. We employ the particle swarm optimization for fixed values of p to find the set of parameters $\{\gamma_j,\beta_j\}$ [38,39]. In the same spirit of Ref. [27], QAOA will be used as a benchmark to check the efficiency of other schemes.

V. TELEPORTATION PROTOCOL

We consider the teleportation protocol introduced in Ref. [29]. In this protocol, there are three qubits under the action of the Hamiltonian (1), where the driving-Hamiltonian is

$$H_0 = -\omega_0\left(\sigma_x^2\sigma_x^3 + \sigma_z^2\sigma_z^3\right), \tag{20}$$

whose ground state is twofold degenerated $|\phi_0^{(1)}\rangle = |0\rangle\otimes|\Phi\rangle$ and $|\phi_0^{(2)}\rangle = |1\rangle\otimes|\Phi\rangle$, where $|\Phi\rangle$ is a Bell state, $|\Phi\rangle = (|00\rangle+|11\rangle)/\sqrt{2}$, and σ_m^j is the Pauli spin matrix in the m direction acting on the jth qubit.

The problem Hamiltonian is

$$H_1 = -\omega_0\left(\sigma_x^1\sigma_x^2 + \sigma_z^1\sigma_z^2\right), \tag{21}$$

whose ground state is also a twofold-degenerated state given by $|\chi_0^{(1)}\rangle = |\Phi\rangle\otimes|0\rangle$ and $|\chi_0^{(2)}\rangle = |\Phi\rangle\otimes|1\rangle$. This protocol aims at teleporting the information initially encoded into the first qubit to the third qubit at the final time of evolution, which is equivalent to a SWAP gate. The fidelity at the final time of evolution T can be evaluated by

$$F(T) = |\langle\psi(T)|\chi_0\rangle|^2, \tag{22}$$

where $|\chi_0\rangle$ can be chosen as any linear combination of states $|\chi_0^1\rangle$ and $|\chi_0^2\rangle$ without loss of generality [29]. As already discussed in Ref. [29], one-qubit gates can be obtained by the unitary transformation of the driving Hamiltonian $H_0' = U_G H_0 U_G^\dagger$, where U_G is the one-qubit gate acting on the third qubit, which can be obtained by local magnetic fields. The same idea can be generalized to implement two-qubit gates. In this case, the Hamiltonian must be extended to a set of six qubits because each subset of three qubits is required to swap the information between the first and the third qubit. Similarly to the one-qubit gates, two-qubit gates are achieved by unitary transformations of the driving Hamiltonian. For instance, the controlled-NOT gate (CNOT) can be accomplished by the rotated driving Hamiltonian such as

$$H_0' = -\omega_0 U_{\mathrm{CNOT}}\left(\sigma_x^2\sigma_x^3 + \sigma_z^2\sigma_z^3 + \sigma_x^5\sigma_x^6 + \sigma_z^5\sigma_z^6\right)U_{\mathrm{CNOT}}, \tag{23}$$

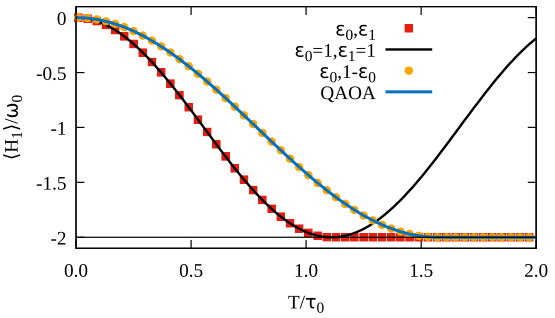

FIG. 1. Mean value $\langle H_1(T)\rangle$ as a function of the final time of evolution, using the first (red dotted curve), the second (black solid curve), the third (orange dotted curve), and the fourth (blue solid curve) time evolution schemes. The thin black horizontal line indicates the smallest eigenvalue of H_1.

where U_{CNOT} is the controlled-NOT gate applied between the third and sixth qubits. The problem Hamiltonian does not depend on the two-qubit gate, thus

$$H_1 = -\omega_0\left(\sigma_x^1\sigma_x^2 + \sigma_z^1\sigma_z^2 + \sigma_x^4\sigma_x^5 + \sigma_z^4\sigma_z^5\right). \tag{24}$$

By setting the ground state of Eq. (23) as the initial state, the time-evolved state up to the minimum time T_{min}, under the total Hamiltonian $H = H_0' + H_1$, is exactly given by $|\psi(T_{\text{min}}\rangle = U_{\text{CNOT}}|\chi_0\rangle$. The unitary gate related to the controlled-NOT can be obtained by evolving the Hamiltonian $H_{\text{CNOT}} = \Delta(\sigma_x^3 + \sigma_z^6) + \Gamma\sigma_x^3\sigma_z^6$, with Δ and Γ being proportional to local magnetic fields and interaction between the third and sixth qubits, respectively. The unitary gate is simply $U_{\text{CNOT}} = \exp(-iH_{\text{CNOT}}T_{\text{min}})$. Furthermore, the Hamiltonian H_{CNOT} can be transformed into a ZZ-type interaction, which is experimentally achievable, by applying a rotation of $\pi/4$ in the y direction to the third qubit, so

$$H_{\text{CNOT}}^R = \Delta(\sigma_z^3 + \sigma_z^6) + J\sigma_z^3\sigma_z^6, \tag{25}$$

where the superscript R indicates the Hamiltonian in the basis rotated by $\pi/4$ in the y direction.

VI. NUMERICAL RESULTS

To probe and compare different approaches, we implement the teleportation protocol using the following temporal evolution schemes: (1) the two-control optimization of $\varepsilon_0(t)$ and $\varepsilon_1(t)$; (2) the double-bang solution $\varepsilon_0(t) = \varepsilon_1(t) = 1$; (3) the one-control optimization, i.e., $\varepsilon_1(t) = 1 - \varepsilon_0(t)$; and (4) the QAOA approach. The linear adiabatic evolution (LAE), where $\varepsilon_0(t) = 1 - t/T$ and $\varepsilon_1(t) = t/T$, is used to initialize the TBQCP method, see Eqs. (15) to (17).

In Fig. 1, we compare the mean value $\langle H_1(T)\rangle = \langle\psi(T)|H_1|\psi(T)\rangle$ as a function of final time T considering different temporal evolution schemes, where $|\psi(T)\rangle$ is the wave function evolved up to the final time by the Hamiltonian defined in Eq. (1). The minimum value of $\langle H_1(T)\rangle$ is achieved in the shorter time for the two-control optimization and the double-bang solution, as shown in Fig. 1. In this case, the mean value $\langle H_1(T)\rangle$ reaches its minimum $-2\omega_0$ for the final time $T = 1.11\tau_0$, where $\tau_0 = \omega_0^{-1}$ is the adopted timescale. The QAOA approach and the one-control optimization essentially have the same performance and achieves the minimum

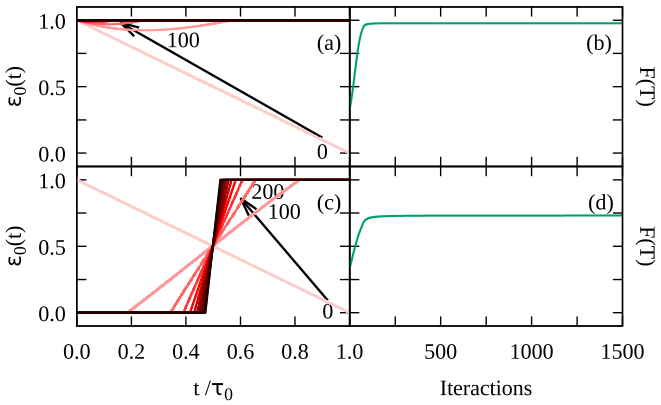

FIG. 2. Panels (a) and (c) show the control $\varepsilon_0(t)$ for 0 to 1400 iterations of the TBQCP method, with a step of 100 iterations, for the second and third schemes, respectively. The number of iterations increases in the direction indicated by the arrows and the color gradient. Thus, the darker the color, the higher the number of iteraction in the TBQCP. Fidelity $F(T)$ as a function of the number of iterations in the TBQCP method, using the second and the third schemes, are shown in panels (b) and (d).

value for final times above $T = 1.57\tau_0$. As demonstrated in Sec. II, when the final time $T \leqslant T_{\text{min}}$, the optimal solution is the double-bang solution. For this type of solution, the mean value can be analytically evaluated $\langle H_1(T)\rangle = -\omega_0[1 - \cos(2\sqrt{2}\omega_0 T)]$, which provides the minimum time $T_{\text{min}} = \frac{\pi}{2\sqrt{2}}\tau_0$. Thus, the mean value $\langle H_1(T)\rangle$ for the double-bang and the two-control optimization coincides up to T_{min}. Although the analytical result for $\langle H_1(T)\rangle$ was obtained by the SWAP gate, this result does not change when either a one- or a two-qubit gate is applied to the physical qubits. Such a result is very interesting because it provides an easy receipt to build an universal quantum computer, which can be summarized as follows: (i) implement the interactions of the Hamiltonians Eqs. (20) and (21) or Eqs. (23) and (24); (ii) build the unitary transformation U_G or C_{NOT} using local magnetic fields and interactions; and (iii) evolve the total Hamiltonian $H = H_0' + H_1$ up to $T_{\text{min}} = \frac{\pi}{2\sqrt{2}}\tau_0$. For the CNOT, the parameters for the H_{CNOT} can be numerically found to implement the gate at $t = T_{\text{min}}$, which are $\Delta = 2.122\omega_0$ and $\Gamma = 0.707\omega_0$.

Within the TBQCP method, we impose bounds on the two-control functions by fixing the functions values in the maximum or minimum bound whenever the functions cross these limits. To better understand this idea, we plot $\varepsilon_0(t)$ considering different iterations of the TBQCP in Fig. 2(a) when the final time is $T = 1.0\tau_0$. The initial trial function (iteration 0) is $\varepsilon_0(t) = 1 - t/T$. After 100 iterations, the function $\varepsilon_0(t)$ starts to bend up, yet does not cross any bound of the interval [0,1]. On the other hand, the TBQCP method finds functions that cross the upper bound after 200 iterations and we force the function to the maximum value within the region where the function found by the TBQCP would cross the upper bound. The function $\varepsilon_0(t)$ becomes constant and reaches the upper bound in the whole time evolution, after 1400 iterations of the TBQCP method. A similar behavior is found to $\varepsilon_1(t)$ (not shown here). In Fig. 2(b), we show the fidelity $F(T)$ as a function of the TBQCP iterations, which converges to 0.9763 after 500 iterations. For all numerical calculations,

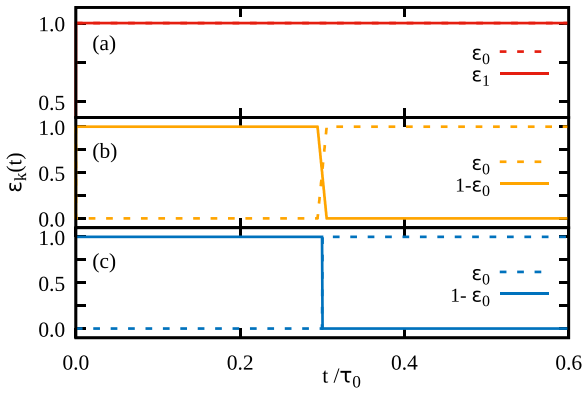

FIG. 3. Optimized controls $\varepsilon_0(t)$ (solid lines) and $\varepsilon_1(t)$ (dashed lines) as a function of time for all considered schemes for the final time $T = 0.6\tau_0$. The two-control optimization, the one-control optimization, and the QAOA scheme are shown in panels (a) to (c), respectively.

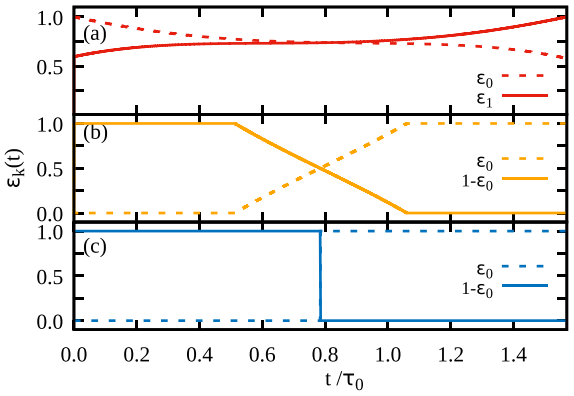

FIG. 5. Optimized fields $\varepsilon_0(t)$ (solid lines) and $\varepsilon_1(t)$ (dashed lines) as a function of time for all considered schemes for the final time $T = 1.8\tau_0$. The two-control optimization, the one-control optimization, and the QAOA scheme are shown in panels (a) to (c), respectively.

we use $\eta = 5 \times 10^{-3}$ in Eq. (17). In Fig. 2(c), we plot the function $\varepsilon_0(t)$ within the one-control optimization scheme as a function of the iterations of the TBQCP method, which cross the bounds after 300 iterations. After 1400 iterations, the function $\varepsilon_0(t)$ resembles a step function, similar to the functions obtained in the QAOA approach. Fidelity $F(T)$ as a function of the TBQCP iterations for the third scheme is shown in Fig. 2(d), which reaches convergence of 0.729 after 1000 iterations.

In Figs. 3–5, we show the converged optimal controls $\varepsilon_0(t)$ (solid lines) and $\varepsilon_1(t)$ (dashed lines) obtained for different final times. In each of these figures, panels (a) to (c) show the controls using the two-control optimization, the one-control optimization, and the QAOA scheme. In Fig. 3(a), we observe that the solution for the two-control optimization using the TBQCP method corresponding to the double-bang solution, which is in perfect accordance to the general results obtained in Sec. II. The one-control optimization and the QAOA provide similar solutions for the controls [Figs. 3(b) and 3(c), which indicates that the QAOA approach with $p = 1$ is very close to the optimal solution for $T = 0.6\tau_0$. It is also interesting to notice that the second scheme, initialized with the smooth linear ramp of LAE, converged to controls of opposite behavior compared to LAE, e.g., $\varepsilon_0(0) > \varepsilon_1(0)$ in the LAE scheme, but $\varepsilon_1(0) > \varepsilon_0(0)$ for the optimized solutions.

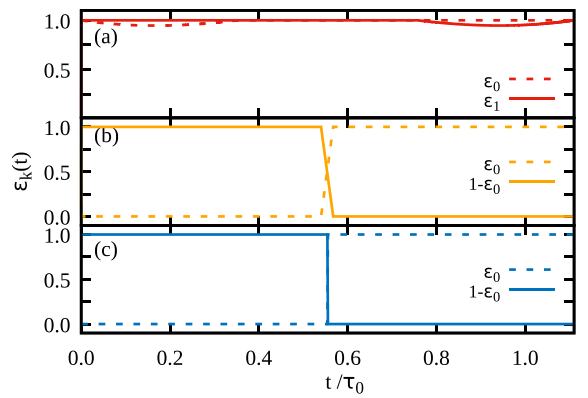

FIG. 4. Optimized fields $\varepsilon_0(t)$ (solid lines) and $\varepsilon_1(t)$ (dashed lines) as a function of time for all considered schemes for the final time $T = 1.11\tau_0$. The two-control optimization, the one-control optimization, and the QAOA scheme are shown in panels (a) to (c), respectively.

In Fig. 4, we plot the resulting controls considering the minimum time $T_{\min} = 1.11\tau_0$. In Fig. 4(a), we observe that the solution for the two-control optimization using the TBQCP is not exactly equal to the double-bang solution, but both solutions are equivalent and give the same value for $\langle H_1(T_{\min})\rangle$. Again, the one-control solution [Fig. 4(b)] is similar to the QAOA approach [Fig. 4(c)] with $p = 1$, where the main difference is the smoother transition between 0 and 1 for the third scheme. Figure 5 shows the control functions for $T = 1.57\tau_0$. In this case, the final time is longer than the minimum time, therefore the two-control optimization converges to solutions different from the double-bang solution. We also notice that the one-control optimization scheme presents a smooth linear transition between the minimum and maximum values of control functions, while the QAOA approach has a jump at $t = 0.785\tau_0$. Although the controls obtained from different schemes have a different temporal evolution, the fidelity is always equal to 1 for $T = 1.57\tau_0$. This result is in agreement with the fact that the control landscape contains infinite optimal solutions [40].

We also perform the analysis of the energetic cost of implementing these different temporal evolution schemes. In Fig. 6, we plot the energy cost as a function of the final time calculated according to Refs. [30,41]:

$$\Sigma(T) = \frac{1}{T}\int_0^T dt||H(t)||, \tag{26}$$

where $||H(t)|| = \sqrt{\mathrm{Tr}\{H(t)^2\}}$. We note that both the QAOA and the double-bang solution have constant energy cost for all T shown in the Fig. 6. This behavior is due to the constant form of the function for these two particular cases. The energetic cost for the two-control optimization and the double-bang solution are the same when $T < 1.11\tau_0$. Above the minimum time, the first scheme presents a lower energetic cost than the double-bang solutions. A similar behavior occurs

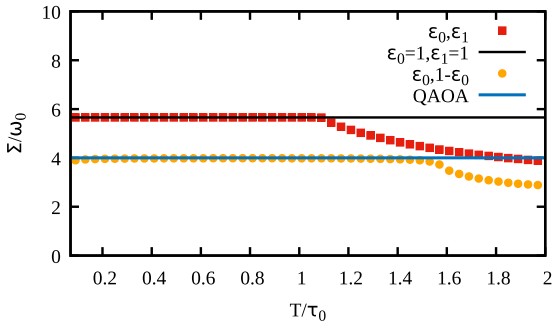

FIG. 6. Energy cost as a function of the final time for the first (red dotted curve), the second (black solid curve), the third (orange dotted curve), and the fourth (blue solid curve) schemes of optimization.

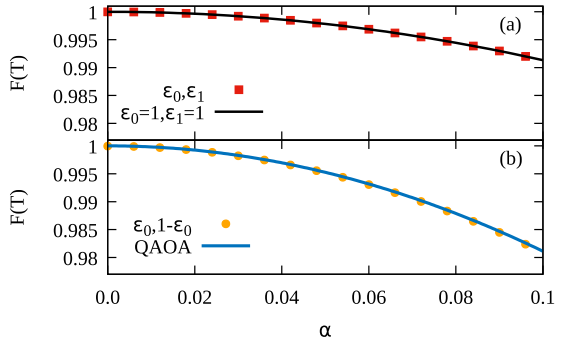

FIG. 7. In panel (a) we plot the fidelity as a function of the magnitude α of the most aggressive type of systematic error considering the first (red dotted curve) and the second (black solid curve) schemes of temporal evolution when $T = 1.11\tau_0$. In panel (b), we plot the fidelity as a function of α for the third (blue solid curve) and the fourth (orange dotted curve) schemes of temporal evolution when $T = 1.57\tau_0$.

when we compare the third and the fourth schemes, i.e., above $T = 1.57\tau_0$, the third scheme has a lower energetic cost than the QAOA approach. The results of Fig. 6 show that solutions found by the TBQCP technique have a lower energy cost when $T > T_{\min}$ because optimal solutions with amplitudes less than the maximum bound are possible in this case.

To probe the robustness of the optimization schemes against systematic errors, we added an error Hamiltonian given by $H_{\text{err}} = \alpha\omega_0\sigma_k^j$ to Eq. (1), where α is proportional to the magnitude of the local magnetic field. We can find the most aggressive type of systematic error by testing all different combinations of σ_k^j and keeping the one that most affects the fidelity. The fidelity in Fig. 7 is evaluated using the optimized controls, but the time evolution is calculated including the error Hamiltonian H_{err} in Eq. (1). The top panel of Fig. 7 shows the fidelity as a function of α considering $T = T_{\min}$ for the two-control optimization and the double-bang solution. For the minimum time $T_{\min} = 1.11\tau_0$, the two-control optimization does not exactly converge to the double-bang solution (see Fig. 4), but both solutions exhibit the same fidelity as a function of the error magnitude α [Fig. 7(a)]. Similarly, the fidelity as a function of α considering $T = 1.57\tau_0$ for the one-control optimization and the QAOA solution display the same dependence of the fidelity as a function of the error magnitude α, as shown in Fig. 7(b). Although all schemes reach the maximum fidelity when $\alpha = 0$, we find that the first and the second schemes are more robust against systematic errors and a 10% of error ($\alpha = 0.1$) causes a reduction of 1.7% in the fidelity.

VII. CONCLUSION

We considered the quantum computing problem of reaching a target state by applying a combination of the problem Hamiltonian and the driving Hamiltonian, each one modulated by an independent control function. We demonstrated that, when the final time is shorter than the minimum time, the optimal solutions are the double-bang solution provided the gradients of the associated control Hamiltonian with respect to controls are nonnegative. This type of solution is very appealing due to its simplicity and the possibility of achieving universal quantum computing in NISQ by means of the AGT protocol. We believe that these findings give a new perspective to perform quantum computation using this architecture, which is at the same time simple and fast. The controls were numerically obtained by the TBQCP method and also by the QAOA approach. We also showed that the use of two controls can generate higher yields than standard QA and QAOA schemes for the same evolution time. Considering the schemes with a single control, we found that QAOA and the optimized control scheme have the same performance and similar bang-bang shape for small final times, but are quite distinct when the final time is sufficient to exactly prepare the target state. Finally, we remark that the double-bang solution is not generally optimal because the corresponding gradients are not always positive. Moreover, there are cases where the gradients are positive, but the double-bang solution will not reach the desired ground state with sufficient precision. However, for certain special systems, the ground state can be obtained with essentially maximum efficiency by using the double-bang solution, as demonstrated in the teleportation protocol. This type of solution, though within a different framework, was also used previously to perform the Grover's algorithm [42]. We believe that the search for the structure of Hamiltonians where the double-bang solution can reach the desired ground state efficiently is a very interesting topic of investigation.

ACKNOWLEDGMENTS

We thank Alan Costa dos Santos and Felipe Fernandes Fanchini for fruitful discussions and suggestions. E.F.d.L. and L.K.C. acknowledges support from the São Paulo Research Foundation, FAPESP (Grants No. 2014/23648-9 and No. 2019/09624-3) and from the National Council for Scientific and Technological Development, CNPq (Grants No. 423982/2018-4 and No. 311450/2019-9).

[1] F. Arute, K. Arya, R. Babbush, D. Bacon, J. C. Bardin, R. Barends, R. Biswas, S. Boixo, F. G. S. L. Brandao, D. A. Buell *et al.*, Nature (London) **574**, 505 (2019).

[2] K. Wright, K. M. Beck, S. Debnath, J. M. Amini, Y. Nam, N. Grzesiak, J.-S. Chen, N. C. Pisenti, M. Chmielewski, C. Collins *et al.*, Nat. Commun. **10**, 5464 (2019).

[3] A. Peruzzo, J. McClean, P. Shadbolt, M.-H. Yung, X.-Q. Zhou, P. J. Love, A. Aspuru-Guzik, and J. L. O'Brien, Nat. Commun. **5**, 4213 (2014).

[4] J. Preskill, Quantum **2**, 79 (2018).

[5] A. Kandala, A. Mezzacapo, K. Temme, M. Takita, M. Brink, J. M. Chow, and J. M. Gambetta, Nature (London) **549**, 242 (2017).

[6] E. Farhi, J. Goldstone, and S. Gutmann, arXiv:1411.4028.

[7] F. Arute, K. Arya, R. Babbush, D. Bacon, J. C. Bardin, R. Barends, S. Boixo, M. Broughton, B. B. Buckley, D. A. Buell *et al.*, Science **369**, 1084 (2020).

[8] V. Dunjko and P. Wittek, Quantum Views **4**, 32 (2020).

[9] M. P. Harrigan, K. J. Sung, M. Neeley, K. J. Satzinger, F. Arute, K. Arya, J. Atalaya, J. C. Bardin, R. Barends, S. Boixo *et al.*, Nat. Phys. **17**, 332 (2021).

[10] J. Lee, A. B. Magann, H. A. Rabitz, and C. Arenz, Phys. Rev. A **104**, 032401 (2021).

[11] M. Cerezo, A. Arrasmith, R. Babbush, S. C. Benjamin, S. Endo, K. Fujii, J. R. McClean, K. Mitarai, X. Yuan, L. Cincio *et al.*, Nat. Rev. Phys. **3**, 625 (2021).

[12] M. Medvidović and G. Carleo, npj Quantum Inf. **7**, 101 (2021).

[13] M. Willsch, D. Willsch, F. Jin, H. De Raedt, and K. Michielsen, Quant. Info. Proc. **19**, 197 (2020).

[14] T. Albash and D. A. Lidar, Rev. Mod. Phys. **90**, 015002 (2018).

[15] R. Barends, A. Shabani, L. Lamata, J. Kelly, A. Mezzacapo, U. L. Heras, R. Babbush, A. G. Fowler, B. Campbell, Y. Chen *et al.*, Nature (London) **534**, 222 (2016).

[16] N. N. Hegade, K. Paul, Y. Ding, M. Sanz, F. Albarrán-Arriagada, E. Solano, and X. Chen, Phys. Rev. Appl. **15**, 024038 (2021).

[17] L. Prielinger, A. Hartmann, Y. Yamashiro, K. Nishimura, W. Lechner, and H. Nishimori, Phys. Rev. Res. **3**, 013227 (2021).

[18] E. J. Crosson and D. A. Lidar, Nat. Rev. Phys. **3**, 466 (2021).

[19] T. Kadowaki and H. Nishimori, Phys. Rev. E **58**, 5355 (1998).

[20] G. E. Santoro, R. Martoňák, E. Tosatti, and R. Car, Science **295**, 2427 (2002).

[21] S. Boixo, T. F. Rønnow, S. V. Isakov, Z. Wang, D. Wecker, D. A. Lidar, J. M. Martinis, and M. Troyer, Nat. Phys. **10**, 218 (2014).

[22] A. Choquette, A. Di Paolo, P. K. Barkoutsos, D. Sénéchal, I. Tavernelli, and A. Blais, Phys. Rev. Res. **3**, 023092 (2021).

[23] C. Lin, Y. Wang, G. Kolesov, and U. C. V. Kalabić, Phys. Rev. A **100**, 022327 (2019).

[24] G. Riviello, K. M. Tibbetts, C. Brif, R. Long, R.-B. Wu, T.-S. Ho, and H. Rabitz, Phys. Rev. A **91**, 043401 (2015).

[25] S. Isermann, Quant. Info. Proc. **20**, 300 (2021).

[26] Z.-C. Yang, A. Rahmani, A. Shabani, H. Neven, and C. Chamon, Phys. Rev. X **7**, 021027 (2017).

[27] L. T. Brady, C. L. Baldwin, A. Bapat, Y. Kharkov, and A. V. Gorshkov, Phys. Rev. Lett. **126**, 070505 (2021).

[28] A. B. Magann, C. Arenz, M. D. Grace, T.-S. Ho, R. L. Kosut, J. R. McClean, H. A. Rabitz, and M. Sarovar, PRX Quantum **2**, 010101 (2021).

[29] D. Bacon and S. T. Flammia, Phys. Rev. Lett. **103**, 120504 (2009).

[30] A. C. Santos, R. D. Silva, and M. S. Sarandy, Phys. Rev. A **93**, 012311 (2016).

[31] D. E. Kirk, *Optimal Control Theory: An Introduction* (Prentice-Hall, Englewood Cliffs, NJ, 1970).

[32] D. Liberzon, *Calculus of Variations and Optimal Control Theory A Concise Introduction* (Princeton University Press, Princeton, NJ, 2012).

[33] U. Boscain, M. Sigalotti, and D. Sugny, PRX Quantum **2**, 030203 (2021).

[34] L. C. Venuti, D. D'Alessandro, and D. A. Lidar, Phys. Rev. Appl. **16**, 054023 (2021).

[35] T.-S. Ho and H. Rabitz, Phys. Rev. E **82**, 026703 (2010).

[36] L. K. Castelano, E. F. de Lima, J. R. Madureira, M. H. Degani, and M. Z. Maialle, Phys. Rev. B **97**, 235301 (2018).

[37] C. M. Rivera-Ruiz, E. F. de Lima, F. F. Fanchini, V. Lopez-Richard, and L. K. Castelano, Phys. Rev. A **97**, 032332 (2018).

[38] J. P. Papa, G. H. Rosa, D. Rodrigues, and Y. Xin-She, arXiv:1704.05174.

[39] I. Sousa-Ferreira and D. Sousa, Journal of Algorithms & Computational Technology **11**, 23 (2016).

[40] H. Rabitz, M. Hsieh, and C. Rosenthal, Phys. Rev. A **72**, 052337 (2005).

[41] S. Deffner, Europhys. Lett. **134**, 40002 (2021).

[42] E. Farhi and S. Gutmann, Phys. Rev. A **57**, 2403 (1998).